Open access • Journal Article • DOI:10.1080/01694243.2012.697783

A comparative study of the morphology and wetting characteristics of micro/nanostructured Cu surfaces for phase change heat transfer applications — Source link

Youngsuk Nam, Y. Sungtaek Ju

Institutions: University of California, Los Angeles

Published on: 28 Aug 2013 - Journal of Adhesion Science and Technology (Routledge)

Topics: Thermal oxidation, Wetting and Contact angle

Related papers:

- Jumping-Droplet-Enhanced Condensation on Scalable Superhydrophobic Nanostructured Surfaces
- Effect of droplet morphology on growth dynamics and heat transfer during condensation on superhydrophobic nanostructured surfaces.
- Self-propelled dropwise condensate on superhydrophobic surfaces.
- Condensation on superhydrophobic copper oxide nanostructures
- Dropwise condensation theory and experiment: A review

Share this paper:

View more about this paper here: https://typeset.io/papers/a-comparative-study-of-the-morphology-and-wetting-474fzzk674

UCLA
UCLA Previously Published Works

Title

A comparative study of the morphology and wetting characteristics of micro/nanostructured Cu surfaces for phase change heat transfer applications

Permalink

https://escholarship.org/uc/item/89h3f2dv

Journal

Journal of Adhesion Science and Technology, 27(20)

ISSN

0169-4243

Authors

Nam, Y
Ju, YS

Publication Date

2013-10-01

DOI

10.1080/01694243.2012.697783

Peer reviewed

eScholarship.org Powered by the California Digital Library
University of California

This article was downloaded by: [University of California, Los Angeles (UCLA)]
On: 18 April 2013, At: 11:16
Publisher: Taylor & Francis
Informa Ltd Registered in England and Wales Registered Number: 1072954 Registered office: Mortimer House, 37-41 Mortimer Street, London W1T 3JH, UK

Journal of Adhesion Science and Technology

Publication details, including instructions for authors and subscription information:
http://www.tandfonline.com/loi/tast20

A comparative study of the morphology and wetting characteristics of micro/nanostructured Cu surfaces for phase change heat transfer applications

Youngsuk Nam [a] [b] & Y. Sungtaek Ju [a]

[a] Department of Mechanical and Aerospace Engineering, University of California, Los Angeles, CA, 90095-1597, USA

[b] Department of Mechanical Engineering, Kyung Hee University, Yongin, 446-701, Korea

Version of record first published: 13 Aug 2012.

To cite this article: Youngsuk Nam & Y. Sungtaek Ju (2012): A comparative study of the morphology and wetting characteristics of micro/nanostructured Cu surfaces for phase change heat transfer applications, Journal of Adhesion Science and Technology, DOI:10.1080/01694243.2012.697783

To link to this article: http://dx.doi.org/10.1080/01694243.2012.697783

PLEASE SCROLL DOWN FOR ARTICLE

Full terms and conditions of use: http://www.tandfonline.com/page/terms-and-conditions

This article may be used for research, teaching, and private study purposes. Any substantial or systematic reproduction, redistribution, reselling, loan, sub-licensing, systematic supply, or distribution in any form to anyone is expressly forbidden.

The publisher does not give any warranty express or implied or make any representation that the contents will be complete or accurate or up to date. The accuracy of any instructions, formulae, and drug doses should be independently verified with primary sources. The publisher shall not be liable for any loss, actions, claims, proceedings, demand, or costs or damages whatsoever or howsoever caused arising directly or indirectly in connection with or arising out of the use of this material.

Journal of Adhesion Science and Technology
2012, 1–14, iFirst article

A comparative study of the morphology and wetting characteristics of micro/nanostructured Cu surfaces for phase change heat transfer applications

Youngsuk Nam[a,b] and Y. Sungtaek Ju[a]*

[a]*Department of Mechanical and Aerospace Engineering, University of California, Los Angeles, CA 90095-1597, USA;* [b]*Department of Mechanical Engineering, Kyung Hee University, Yongin 446-701, Korea*

(*Received 7 October 2010; final version received 8 October 2011; accepted 22 September 2011*)

A comparative study of oxidation methods to create Cu surfaces with controlled wettability is reported. Micro/nanostructures of Cu oxides are formed on Cu substrates using different chemical and thermal oxidation methods. The morphology and wetting characteristics of the resulting surfaces are characterized using atomic force microscopy, scanning electron microscopy, X-ray diffraction, and contact angle measurements. Chemical oxidation in alkali solutions can form uniform copper oxide layers with high roughness factors without causing thermal stress problems that often hamper thermal oxidation. By combining chemical oxidation with a hydrophobic coating, a wide range of wettability control is demonstrated from superhydrophilic ($\theta_a < 10°$) to superhydrophobic ($\theta_a > 170°$). Superhydrophilic CuO layers uniformly formed on Cu powder and Cu micropost wick surfaces lead to significant improvement in the capillary and heat transfer performance compared with comparable unoxidized Cu wicks. The present work motivates further studies to exploit the benefits of nanostructured Cu surfaces in various phase change heat transfer applications.

Keywords: wetting; cupric oxide; oxidation; capillary; wick; superhydrophilic

1. Introduction

Previous studies [1–3] have identified surface wettability as one of the key factors affecting phase change heat transfer. Significant enhancement in the critical heat flux, for example, has been reported for Cu plates coated with superhydrophilic TiO_2 layers in both pool boiling [2] and water jet impingement cooling experiments [3]. The performance of wicks in heat pipes can also benefit from enhanced wettability. The heat transfer capacity of heat pipes is often determined by the capillary limit, where the sum of liquid and vapor pressure drops exceeds the maximum capillary pressure of the wick. The capillary limit for a heat pipe in horizontal orientation is approximately given as [4]:

$$(Q_{\max})_{\phi=0} = 2 \cdot \left(\frac{\rho_l \sigma_{lg} h_{lg}}{\mu_l}\right) \cdot \left(\frac{K}{R_{\text{eff}}}\right) \cdot \frac{A_w}{L_{\text{eff}}}, \quad R_{\text{eff}} = \frac{r_p}{\cos\theta_s}. \tag{1}$$

*Corresponding author. Email: just@seas.ucla.edu

ISSN 0169-4243 print/ISSN 1568-5616 online
© 2012 Taylor & Francis
http://dx.doi.org/10.1080/01694243.2012.697783
http://www.tandfonline.com

Downloaded by [University of California, Los Angeles (UCLA)] at 11:16 18 April 2013

Downloaded by [University of California, Los Angeles (UCLA)] at 11:16 18 April 2013

The combination of the fluid properties is called the merit number. The second factor (K/R_{eff}) represents the capillary performance determined by the geometry and wettability of the wick. Here, K is the permeability and R_{eff} is the effective pore radius. The capillary performance can be enhanced by using low surface energy liquids such as methanol, but the merit number of most well-wetting liquids is often an order of magnitude smaller than that of water.

Localized hydrophobic regions on an otherwise hydrophilic surface may also be beneficial for certain phase change heat transfer applications as they facilitate controlled nucleation and growth of vapor bubbles. Enhanced nucleate boiling in early stages of boiling has been reported on hydrophobic [5,6] and superhydrophobic surfaces [7]. Sustained bubble nucleation at superheat below 2 K was observed on a superhydrophobic surface with a contact angle approximately 150° [7]. A previous study of bubble-based microactuators also reported that localized hydrophobic regions allow reduction in the superheat required for reliable bubble nucleation [6].

Although previous studies demonstrated the benefits of enhanced wetting for phase change heat transfer applications, major challenges still lie in developing practical heating surfaces with high wettability, high thermal and temporal stability, low parasitic thermal resistance, and low fabrication cost. TiO_2-based coatings used in previous heat transfer studies [2,3], for example, gradually lose their superhydrophilicity in the absence of UV irradiation [8].

As described by the Wenzel [9] and Cassie–Baxter [10] models, the wettability of a surface can be tuned by changing its morphology as well as surface energy. In the Wenzel regime, a liquid fills the grooves of a rough surface, which reduces the effective contact angle according to the following equation:

$$\cos\theta_a = r\cos\theta_s. \tag{2}$$

In the Cassie regime, gas pockets are formed underneath a liquid drop, effectively forming a composite surface made of the gas and the solid. The apparent contact angle is then governed by the chemical heterogeneity of the surface as:

$$\cos\theta_a = f_s\cos\theta_s + (1-f_s)\cos\theta_c. \tag{3}$$

Copper is one of the most attractive structural materials for heat transfer applications due to its high thermal conductivity, favorable processing properties, and relatively low price. Water is the most common operating liquid due to its high enthalpy of vaporization, ease of handling, and low price. The wettability of water on copper surfaces, however, is relatively poor. The static contact angle of water droplets on air-exposed Cu often exceeds 70°.

Thermal or chemical oxidation of Cu is a convenient way to alter both its surface energy and morphology. Recent studies reported the synthesis of various cupric oxide (CuO) nanostructures with different morphologies, such as sharp needle-like nanowires [11,12], nanobelts [13], nano-rods and ribbons [14–16], and 3D flower-like networks [17] using chemical oxidation schemes. Thermal oxidation is another route to synthesize micro- and nanostructures of copper oxides. At heating temperatures below 260 °C, Cu_2O layers are typically formed on pure Cu substrate [18,19]. For heating temperatures between 400 and 700 °C, CuO nanowires of 10–200 nm in diameter are synthesized [20,21].

In the present article, we report our comparative study of copper oxidation methods. We perform detailed characterization of the surface morphology and wettability of copper oxide structures formed by different thermal and chemical oxidation methods. We demonstrate the ability to tune the wettability of Cu surfaces from superhydrophilic to superhydrophobic. A selected oxidation scheme is applied to form superhydrophilic Cu wick structures to demon-

strate that their capillary and heat transfer performance is significantly improved compared to comparable unoxidized wicks.

2. Experimental procedure

We used commercially available copper foils (99.9% purity, 0.8 mm thickness, and 2 cm × 2 cm size) as starting substrates. Each substrate was polished with 200, 400, 600, 800, and 1200 grit sandpapers and alumina particles of 1 μm diameter. The substrate was cleaned in an ultrasonic bath with acetone for 20 min and rinsed with deionized (DI) water. The substrate was then dipped into a 2.0 M hydrochloric acid solution for 30 s to remove preexisting oxide layers, rinsed with DI water, and dried in a nitrogen blow.

For chemical oxidation processes, each clean copper substrate was immersed in a hot alkali solution. After a specific time, the specimen was removed from the solution, rinsed in deionized water five times, and dried in a nitrogen blow for characterization. Table 1 lists the detailed information on different alkali solutions used in the present study. To distinguish oxide micro/nanostructures obtained from the different alkali solutions, we label them as Type I, II, and III oxide nanostructures, respectively. For thermal oxidation processes, Cu substrates were heated under atmospheric conditions using a hot plate (for the temperature range of 150–250 °C) or a box furnace (for the temperature range of 400–800 °C).

The surface morphology and roughness of the oxide micro- and nanostructures were characterized using contact mode atomic force microscopy (AFM) (PSIA, XE-100) and scanning electron microscopy (SEM) (Hitachi, S4700). X-ray diffraction (XRD) measurements were also performed to determine the chemical compositions of the oxide layers. The static contact angle of a water droplet (4 μL) on each oxidized specimen was measured using a goniometer (First Ten Angstroms, FTÅ 4000A). Droplets were placed on three different spots on each sample and the image analysis was repeated five times at each spot.

3. Results and discussion

3.1. Morphology of CuO nanostructures

Figure 1 shows the SEM images of Types I–III CuO nanostructures. In the case of Type I CuO (Figure 1(a) and (b)), a thin (~200 nm) Cu_2O layer initially covers the substrate and then sharp CuO nanostructures start to grow after approximately 1 min on the Cu_2O intermediate layer. A dense array of sharp CuO nanostructures covers the entire surface at approximately 5 min. The oxide growth rate significantly slows down to an almost negligible level after that the CuO layer passivates the copper surfaces [22]. The XRD result (Figure 2, Type I) shows a strong CuO peak originating from the oxide nanostructures and a weak Cu_2O peak originating from the underlying thin Cu_2O layer. The height of the oxide nanostructures is

Table 1. Chemical composition and temperature of the alkali solutions used in the chemical oxidation processes.

	Type I [11]	Type II [12]	Type III [17]	
$NaClO_2$	3.75 g	16 g	NH_4OH aqueous solution	10 mM–1 M
NaOH	5 g	1 g		
$Na_3PO_4 \cdot 12H_2O$	10 g	–		
DI water	100 mL	100 mL		
Temperature	95 °C	70 °C	60 °C	

Downloaded by [University of California, Los Angeles (UCLA)] at 11:16 18 April 2013

Downloaded by [University of California, Los Angeles (UCLA)] at 11:16 18 April 2013

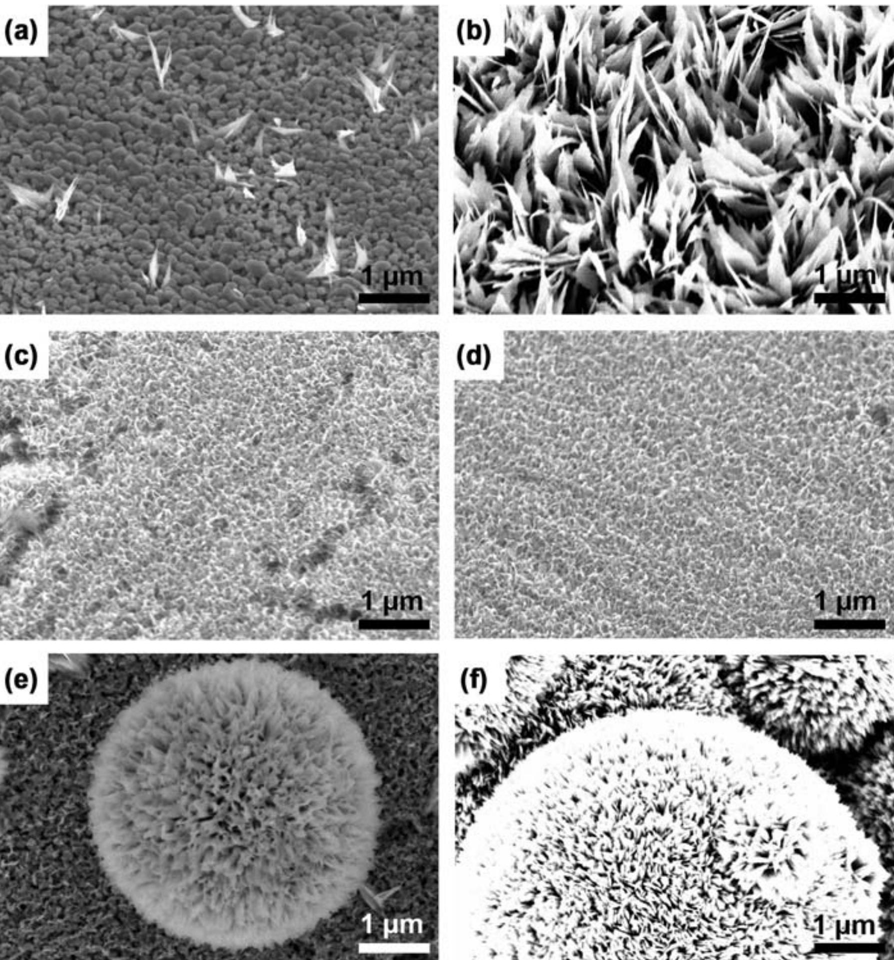

Figure 1. SEM images of CuO nanostructures, (a) and (b) Type I after 1 min (a) and 5 min (b) of oxidation; (c) and (d) Type II after 1 min (c) and 3 min of oxidation (d); and (e) and (f) Type III after 100 min in 60 mM (e) and 8 h in 1 M (f) of aqueous NH_4OH solutions.

~1 μm after approximately 5 min of growth, which is consistent with previous results obtained using the galvanostatic reduction method [23].

By changing the chemical composition of a hot alkali solution, we can grow oxide micro/nanostructures of different morphologies. Type II CuO nanostructures (Figure 1(c) and (d)) have a similar shape as Type I CuO nanostructures, but their height (~200 nm) is about five times smaller. Type II CuO nanostructures grow uniformly over the entire exposed Cu surface for approximately 3 min. After that, no discernible additional growth is observed in SEM measurements.

3D hierarchical oxide structures (Type III) are synthesized in an NH_4OH solution heated at 60 °C. At this and higher temperatures, $Cu(OH)_2$ is first formed and then converted into CuO. The tested range of NH_4OH concentrations (10 mM–1 M) in the present study is much wider than the range reported in the previous study [17]. At the lowest concentration (10 mM), only 2D nanosheet arrays are formed. When the concentration is increased to 60 mM, spherical 3D hierarchical structures start to form (Figure 1(e)). At still higher concen-

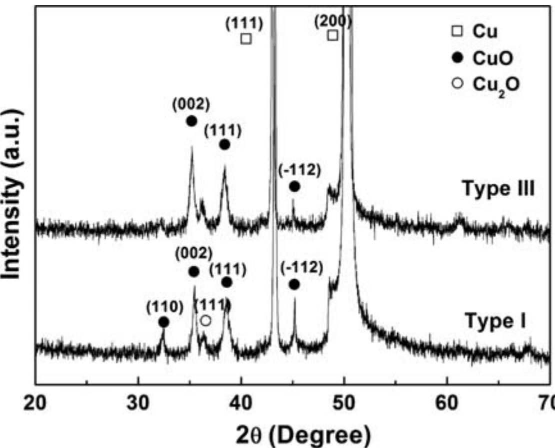

Figure 2. XRD patterns of Type I and III copper oxide structures formed using chemical oxidation methods.

Downloaded by [University of California, Los Angeles (UCLA)] at 11:16 18 April 2013

trations (Figure 1(f)), the oxide structures become thicker and their morphology become more complex as copper ions can reach the supersaturation level for nucleation in much shorter times [17]. Unlike Type I or II oxide structures, we do not observe any apparent self-limiting behavior. Increasing the oxidation time leads to further increases in the thickness and complexity of the oxide structures. The XRD result (Figure 2, Type III) confirms that $Cu(OH)_2$ is converted into CuO during the oxidation process.

In order to compare the above chemical oxidation schemes with more conventional thermal oxidation schemes, clean copper substrates were thermally oxidized at different temperatures for different times in the air. Equation (4) shows the chemical reactions involved in thermal oxidation.

$$4Cu + O_2 \rightarrow 2Cu_2O$$

$$2Cu_2O + O_2 \rightarrow 4CuO. \tag{4}$$

In the initial stage of thermal oxidation, a Cu_2O layer first grows. Only when the Cu_2O layer reaches a critical thickness and the heating temperature is over ~260 °C, a CuO layer is formed. The critical thickness was measured to be between 90 and 300 nm [19,20].

For one set of copper samples, we heated the samples at relatively low temperatures (150–250 °C) for different times (10 min–4 h). Under these conditions, only Cu_2O layers are formed. Figure 3 shows the surface topography after 1 h of heating at different temperatures. Changes in rms roughness during the thermal oxidation processes are shown in Figure 4. The surface roughness was measured using AFM on three different spots for each sample and the error bars represent the standard deviations. Higher heating temperatures result in larger Cu_2O grains, increasing the rms roughness.

Another set of samples was heated at temperatures ranging from 400 to 700 °C. As shown in Figure 5, CuO nanowires start growing on top of initially formed Cu_2O layers after approximately 1 h of heating at 400 °C. Previous studies [20] reported that the heating temperature and time determined the diameter and length of nanowires, respectively. When the heat-

Downloaded by [University of California, Los Angeles (UCLA)] at 11:16 18 April 2013

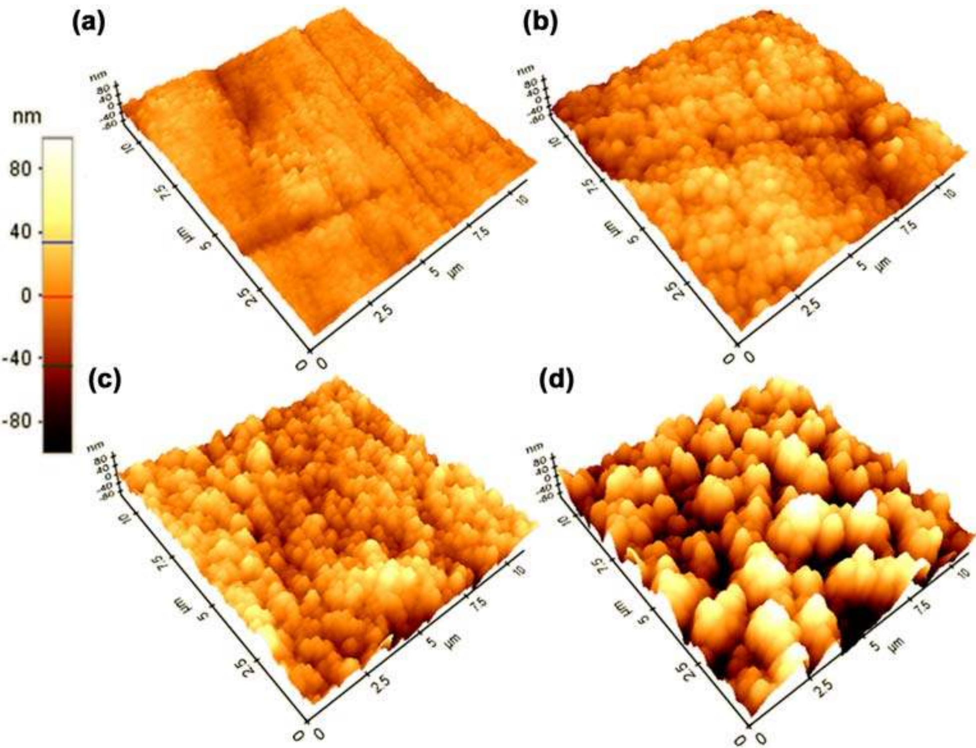

Figure 3. Surface topography of (a) polished copper before heating; (b–d) Cu_2O layer thermally grown for 1 h at 150 °C (b), 200 °C (c), and 250 °C (d). Color map represents *z*-level.

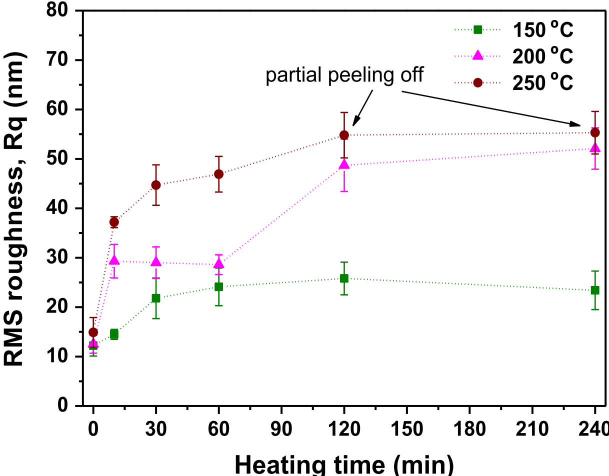

Figure 4. Changes in the rms roughness during thermal oxidation. Copper oxide layers grown at high temperature (250 °C) over 120 min were partially peeled off from the substrates.

ing temperature is raised to 800 °C, significant growth in oxide grains is observed (Figure 5 (d)). Due to large thermal stress, copper oxide layers thermally grown at such elevated temperatures can readily peel off from the substrates, limiting their use in practical applications.

Downloaded by [University of California, Los Angeles (UCLA)] at 11:16 18 April 2013

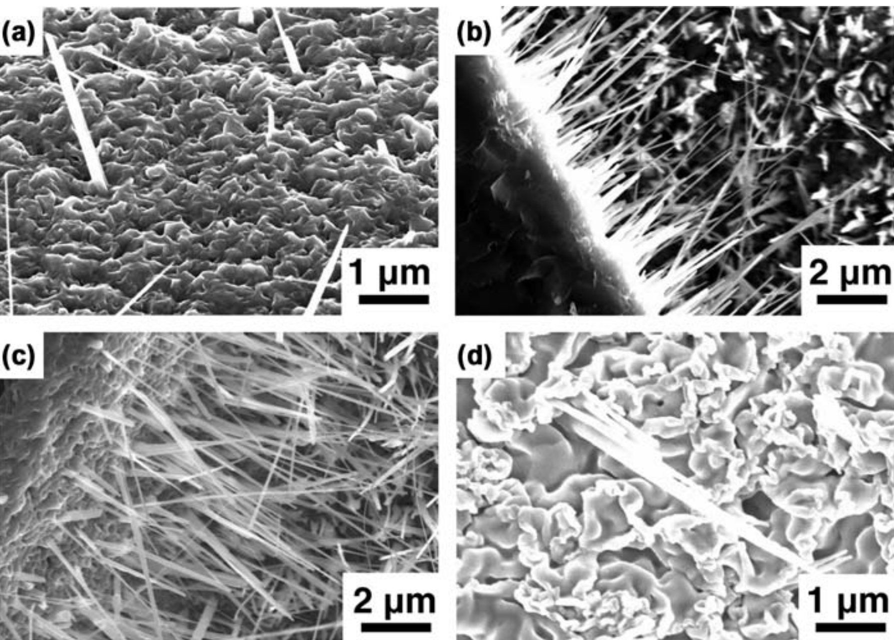

Figure 5. SEM images of CuO nanowires synthesized through thermal oxidation at (a) 400 °C for 1 h, (b) 500 °C for 1 h, (c) 500 °C for 4 h, and (d) 800 °C for 4 h.

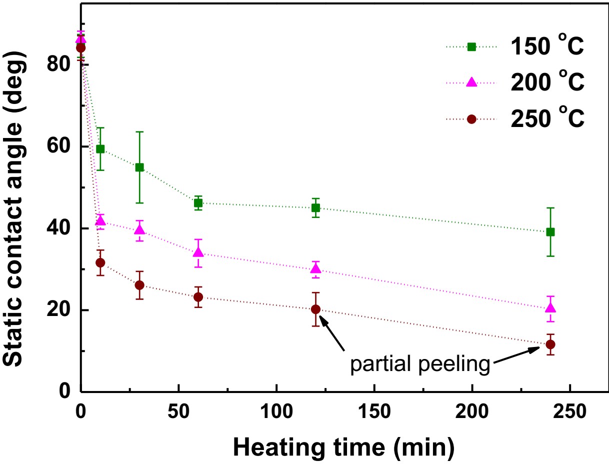

Figure 6. Static contact angles measured on Cu surfaces thermally oxidized at different temperatures. Copper oxide layers grown at high temperature (250 °C) over 120 min were partially peeled off from the substrates.

3.2. Contact angle of water droplets on micro/nanostructured cu surfaces

Figure 6 shows changes in the static contact angle for the samples thermally oxidized at temperatures 150–250 °C for 10 min–4 h. By varying the heating temperature and time, we can modify the contact angle from approximately 90°–15°. When the copper substrates are oxi-

Downloaded by [University of California, Los Angeles (UCLA)] at 11:16 18 April 2013

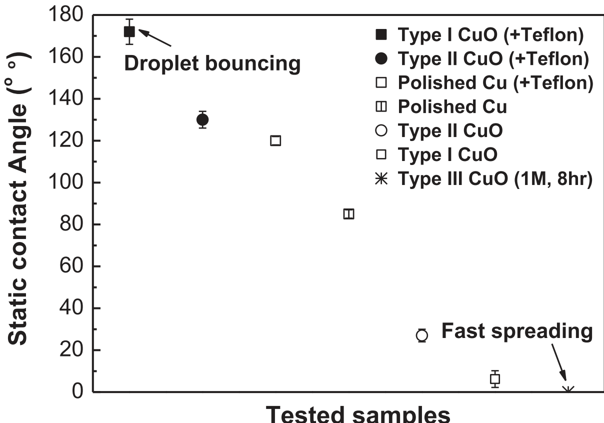

Figure 7. Static contact angles measured on Cu surfaces chemically oxidized in the alkaline solutions listed in Table 1.

dized at relatively low temperatures (150 °C), the increase in surface roughness is rather moderate (see Figure 3). The decrease in contact angle is mainly due to the high surface energy of the copper oxides. At higher heating temperatures, increase in the surface roughness leads to further decrease in the contact angle.

Figure 7 shows the static contact angles for the chemically oxidized Cu surfaces. The contact angle decreases from approximately 90°–6° after 5 min of oxidation for Type I CuO nanostructures and to approximately 25° after 3 min of oxidation for Type II CuO nanostructures. For Type III oxide layers formed in a 1 M NH_4OH solution for 8 h, the droplet spreads instantaneously over the sample surface due to their extremely high roughness factor.

When combined with a thin (<50 nm) hydrophobic coating, such as that of Teflon®, the Cu oxide nanostructures can also provide extreme hydrophobicity as the wetting mode changes from the Wenzel to the Cassie regime. A 2% (by weight) Teflon amorphous fluoropolymer resin (Du Pont Polymers, Inc.) was first dissolved in a FC 40 solvent (3 M). The solution was spin coated on the oxidized Cu surfaces at 3000 rpm for 30 s and then baked at 180 °C for 10 min to evaporate the solvent. The sharp needle-like structures of Type I CuO lead to extreme nonwetting characteristics ($\theta_a > 170°$) by trapping air pockets underneath a water droplet. We note that such hydrophobic coatings may induce morphology changes, especially for Type II CuO structures whose length scale is of the order of 200 nm.

3.3. Integration into wicks

Based on our comparative study, Type I CuO nanostructures were selected for integration into wicks for potential applications in heat pipes and other heat exchangers that utilize phase change heat transfer. Type III nanostructure, despite its high wettability, is deemed ill-suited for integration into complex microporous wick structures as the associated oxidation process is not self-limiting, making it difficult to control the resulting oxide thickness.

The unique needle-like morphology of Type I CuO provides extreme wettability to Cu surfaces without introducing significant parasitic thermal resistance. When Type I CuO nanostructures are integrated onto the surface of the wicks, a thin (<200 nm) Cu_2O layer forms first and sharp needle-like CuO nanostructures are separately grown on this layer (see Figure 1 (a) and (b)). The thermal resistance of the thin continuous underlayer is estimated to be of the order of 10^{-7} m^2 K/W, which is orders of magnitude smaller than the overall thermal

resistance in typical pool boiling conditions. Since the oxidation process is quasi-self-limiting, we can form uniform Type I CuO oxide layers over complex microstructures.

We demonstrated the integration of Type I CuO nanostructures into Cu powder and microfabricated post wicks. The powder wicks were fabricated by sintering Cu powder of diameter approximately 60 μm and the micropost wicks were microfabricated using the electrochemical deposition technique [24].

Figure 8 shows that one can indeed form uniform Type I CuO nanostructures over the entire surface of the monolayer powder and the micropost wicks. Due to the extreme wettability of the CuO nanostructures, poorly wetting copper wicks are turned into superhydrophilic wicks. To characterize the capillary performance of these wicks, we performed capillary rate of rise experiments [24–26] before and after integrating CuO nanostructures. A wick sample is oriented perpendicular to the horizontal surface of a liquid reservoir and slowly lowered using a z-stage. Once the bottom of the wick touches the reservoir surface, the liquid rises along the wick due to a finite capillary pressure gradient. The liquid rise can be described by balancing among the capillary force, the viscous force, and the gravity.

$$\frac{2\sigma_{\mathrm{lg}}}{R_{\mathrm{eff}}} = \frac{\varepsilon}{K}\mu x\frac{\mathrm{d}x}{\mathrm{d}t} + \rho g x. \tag{5}$$

The measured liquid rise history is fitted using Equation (5) to determine the capillary performance parameter K/R_{eff}. The results are summarized in Figure 9. Each measurement was repeated multiple times and the error bars represent the standard deviations. A small effective pore radius R_{eff} leads to high capillary pressure, but it also decreases the permeability K. The ratio K/R_{eff} captures the trade-off between these two competing effects. Methanol is used as a

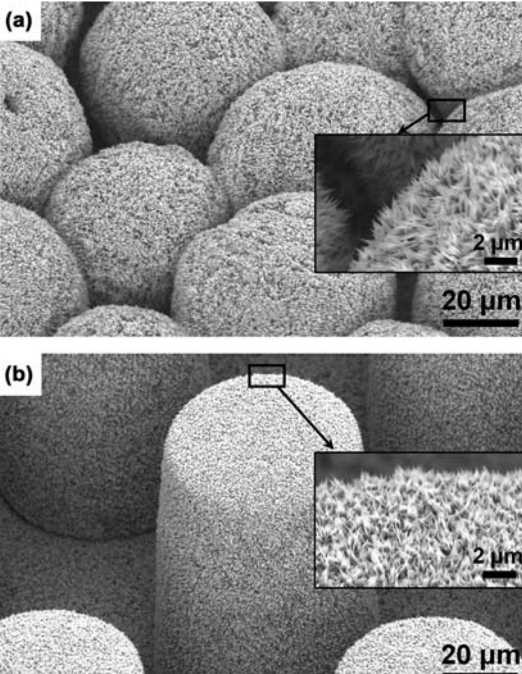

Figure 8. SEM images of nanostructured Cu wicks: (a) monolayer powder wick and (b) microfabricated post wick.

Downloaded by [University of California, Los Angeles (UCLA)] at 11:16 18 April 2013

test liquid for the unoxidized wicks since no self-initiated capillary rise is observed with water due to its high contact angle on bare Cu surfaces. To facilitate comparison with the oxidized wicks, the results obtained with methanol were converted into equivalent values for water (labeled as 'prediction' in Figure 9) using the measured contact angle ($R_{\mathrm{eff}} = r_{\mathrm{p}}/\cos\theta$).

Figure 9 shows that the capillary performance (for water) is enhanced by almost an order of magnitude compared with the bare wick for both the monolayer powder and the micropost wicks. For these nanostructured wicks, the wicking performance with water is approximately equal to the performance with methanol.

Downloaded by [University of California, Los Angeles (UCLA)] at 11:16 18 April 2013

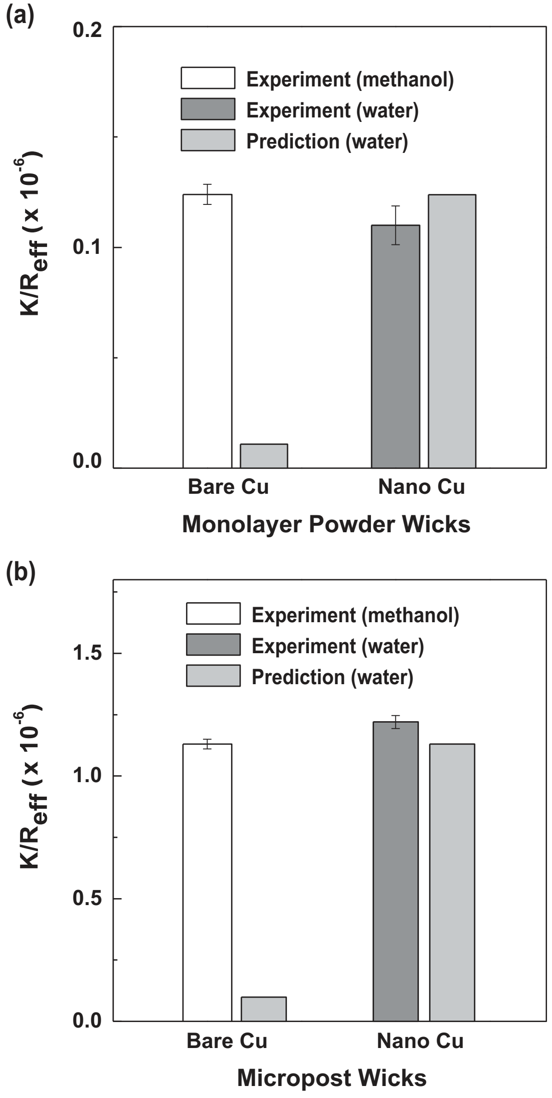

Figure 9. Capillary performances (K/R_{eff}) before and after nanostructuring: (a) monolayer powder wicks and (b) microfabricated post wicks. Methanol and water were used as test liquids. For the unoxidized wicks, the results obtained with methanol were converted into equivalent values for water and labeled as 'prediction.'

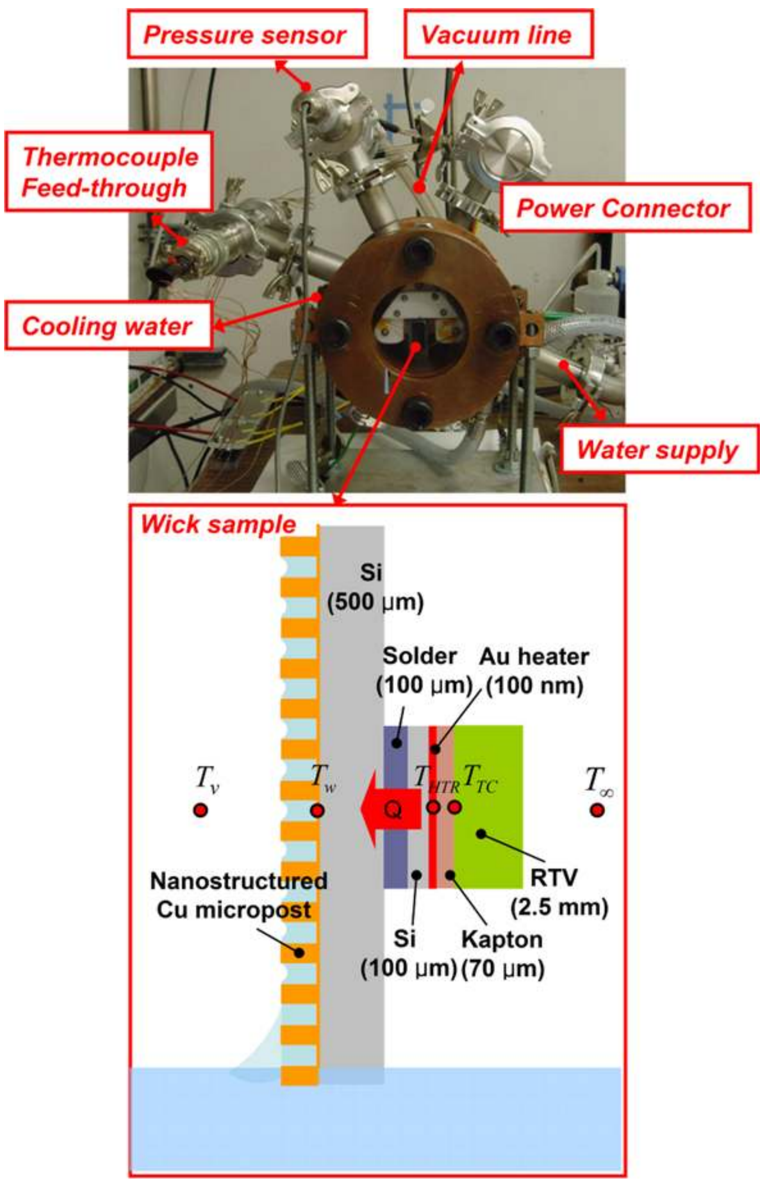

Figure 10. The photograph of the vacuum system used for the heat transfer performance tests (top) and the schematic of the wick sample with an installed heater chip (bottom).

In order to quantify the benefits of nanostructured superhydrophilic surfaces in phase change heat transfer, evaporative heat transfer performance tests were conducted on microfabricated wick samples before and after integrating the CuO nanostructures. Figure 10 shows the vacuum chamber used in the tests and the schematic of the tested wick samples. Cooling water from a thermal bath (Thermoscientific, RTE 7) is circulated around the chamber to precisely maintain the temperature inside the chamber. Vacuum feed-throughs are integrated into the chamber to connect the thermocouple wires and heater lead wires to a data acquisition system and power supply (Agilent, N5752A). The voltage drop across the heater is measured using a separate pair of sensing wires using a multimeter (Keithley, model 2000). To

Downloaded by [University of California, Los Angeles (UCLA)] at 11:16 18 April 2013

Downloaded by [University of California, Los Angeles (UCLA)] at 11:16 18 April 2013

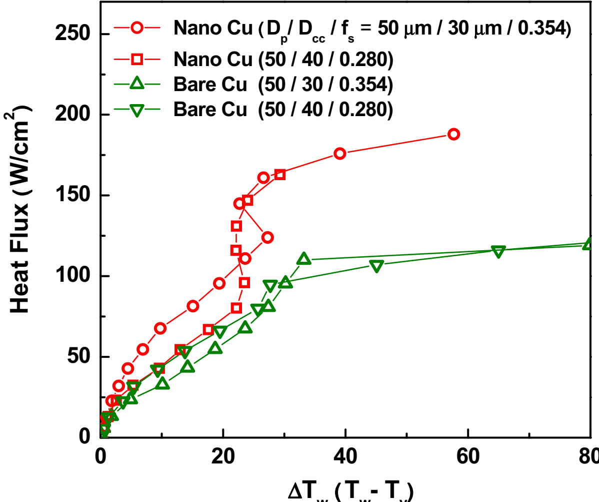

Figure 11. Heat flux as a function of the wick superheat ($T_w - T_v$) before and after the surfaces of the microposts are nanostructured. In the label, D_p (post diameter, µm), D_{cc} (post spacing, µm), and f_s (solid fraction).

mitigate difficulties in controlling the liquid fill charge [27,28], we placed the wick sample perpendicular to the water reservoir. The wick sample is self-saturated via capillary force, which prevents flooding of the wick surface.

A thin-film heater of size 5 mm × 5 mm was fabricated on a silicon substrate of 100 µm thickness. The heater chip was soldered to the backside of the wick sample as a heat source. The thermal resistance of the solder interface between the heater chip and the sample was measured to be 5×10^{-7} m^2 K/W using the transient hot disk technique [29].

We determined the temperature of the heater from its electrical resistance and also from readings of a small (36 AWG) K-type thermocouple bead bonded to the heater surface using a high thermal conductivity epoxy (Omega, Omegabond 101). From the heater temperature, the wall temperature of the wick (T_w) was determined using numerical simulations accounting for heat spreading within the substrate and the heater chip. Further experimental details are provided in a separate publication [29].

Figure 11 shows the heat transfer performance before and after the nanostructuring. At low heat fluxes (<25 W/cm^2), the heat transfer performance stays approximately the same even after the nanostructuring. This suggests that the parasitic thermal resistance associated with the CuO layers is indeed negligible. At higher heat fluxes, the heat transfer performance of the nanostructured wick samples exceeds that of the bare Cu wick samples as the improved capillary performance delays partial dry out. The critical heat flux is enhanced by over 70%, consistent with the significant increase we observed in the capillary performance. These results suggest that the benefits of nanostructured superhydrophilic surfaces may outweigh the potential drawbacks, i.e. parasitic thermal resistance of the oxide layers.

4. Summary and conclusion

We compare the oxidation methods for controlling the morphology and wetting characteristics of copper surfaces. The ability to achieve wide ranges of wettability, from superhydrophilic ($\theta_a < 10°$) to superhydrophobic ($\theta_a > 170°$), is demonstrated. Quasi-self-limiting behavior

allows us to integrate CuO nanostructures into complex microstructures, including monolayer powder and micropost wicks, using a simple wet chemical process. The unique morphology and high surface energy of the CuO nanostructures turn poorly wetting Cu wicks into superhydrophilic wicks without introducing significant parasitic thermal resistance. The CuO nanostructuring significantly enhances both capillary and heat transfer performances. Our work suggests a promising approach to enhancing phase change heat transfer performance by fully benefiting from the high merit number of water without sacrificing the capillary performance.

Nomenclature

A_w	(cross-sectional) area of wick (m^2)
D_{cc}	post spacing (μm)
D_p	post diameter (μm)
f_s	area fraction of solid
g	gravitational acceleration (m/s^2)
h_{lg}	latent heat of vaporization (J/kg)
L_{eff}	effective length of heat pipe (m)
K	permeability (m^2)
Q_{max}	maximum heat transfer capacity (W)
r	roughness factor
r_p	pore radius (m)
R_{eff}	effective radius (m)
t_c	calculated time (s)
t_m	measured time (s)
T_v	vapor temperature (°C)
T_w	wick temperature (°C)
x	liquid rising height (m)

Greek symbols

ε	porosity
ϕ	orientation angle (°)
μ_l	liquid viscosity (Pa s)
m	figure of merit (W/m^2)
θ_c	contact angle of composite surface (°)
θ_s	contact angle of smooth surface (°)
θ_a	apparent contact angle (°)
ρ	density (kg/m^3)
σ_{lg}	liquid–gas (vapor) surface tension (N/m)

References

[1] Dhir VK. Mechanistic prediction of nucleate boiling heat transfer-achievable or a hopeless task? Journal of Heat Transfer. 2006;128:1.

[2] Takata Y, Hidaka S, Masuda M, Ito T. Pool boiling on a superhydrophilic surface. International Journal of Energy Research. 2003;27:111.

[3] Liu Z, Qiu Y. Critical heat flux of steady boiling for water jet impingement in flat stagnation zone on superhydrophilic surface. Journal of Heat Transfer. 2006;128:726.

[4] Mills AF. Heat transfer. Boston, MA: Irwin Press; 1992. 680.

[5] Nam Y, Wu J, Warrier G, Ju YS. Experimental and numerical study of single bubble dynamics on a hydrophobic surface. Journal of Heat Transfer. 2009;131:121004.

Downloaded by [University of California, Los Angeles (UCLA)] at 11:16 18 April 2013

[6] Maxwell RB, Gerhardt AL, Gray ML, Schmidt MA. A microbubble-powered bioparticle actuator. Journal of Microelectromechanical Systems. 2003;12:630.
[7] Takata Y, Hidaka S, Uraguchi T. Boiling feature on a super water-repellent surface. Heat Transfer Engineering. 2006;27:25.
[8] Wang R, Hashimoto K, Fujishima A, Chikuni M, Kojima E, Kitamura A, Shimohigoshi M, Watanabe T. Light-induced amphiphilic surfaces. Nature. 1997;388:431.
[9] Wenzel RN. Resistance of solid surfaces to wetting by water. Industrial and Engineering Chemistry. 1936;28:988.
[10] Cassie ABD, Baxter S. Wettability of porous surfaces. Transactions of the Faraday Society. 1944;40:546.
[11] Yun HK, Cho K, An JH, Park CE. Adhesion improvement of copper/epoxy joints. Journal of Materials Science. 1992;27:5811.
[12] Love BJ, Packman PF. Effects of surface modifications on the peel strength of copper-based polymer/metal interfaces with characteristic morphologies. Journal of Adhesion. 1993;40:139.
[13] Song X, Yu H, Sun S. Single-crystalline CuO nanobelts fabricated by a convenient route. Journal of Colloid and Interface Science. 2005;289:588.
[14] Wen XG, Zhang WX, Yang SH. Synthesis of $Cu(OH)_2$ and CuO nanoribbon arrays on a copper surface. Langmuir. 2003;19:5898.
[15] Wen XG, Xie Y, Choi CL, Wan KC, Li XY, Yang S. Copper-based nanowire materials: templated syntheses, characterizations, and applications. Langmuir. 2005;21:4729.
[16] Tang K, Wang X, Yan W, Yu J, Xu R. Fabrication of superhydrophilic Cu_2O and CuO membranes. Journal of Membrane Science. 2006;286:279.
[17] Liu J, Huang X, Li Y, Sulieman KM, He X, Sun F. Hierarchical nanostructures of cupric oxide on a copper substrate: controllable morphology and wettability. Journal of Materials Chemistry. 2006;16:4427.
[18] Tylecote RF. The composition and reduction of oxide films on copper. Metallurgia. 1956;53:191.
[19] Young FW, Cathcart JV, Gwathmey AT. The rates of oxidation of several faces of a single crystal of copper as determined with elliptically polarized light. Acta Metallurgica. 1956;4:145.
[20] Jiang X, Herricks T, Xia Y. CuO nanowires can be synthesized by heating copper substrates in air. Nano Letters. 2002;2:1333.
[21] Xu CH, Woo CH, Shi SQ. Formation of CuO nanowires on Cu foil. Chemical Physics Letters. 2004;399:62.
[22] Drogowsak M, Brossard L, Ménard H. Influence of anions on the passivity behavior of copper in alkaline solutions. Surface and Coatings Technology. 1988;34:383.
[23] Lee HY. A study on the adhesion of lead frame to EMC [PhD thesis]. Daejeon: Korea Advanced Institute of Science and Technology; 1999.
[24] Nam Y, Sharratt S, Byon C, Kim SJ, Ju YS. Fabrication and characterization of the capillary performance of superhydrophilic Cu micropost arrays. Journal of Microelectromechanical Systems. 2010;19:581.
[25] Holley B, Faghri A. Permeability and effective pore radius measurements for heat pipe and fuel cell applications. Applied Thermal Engineering. 2006;26:448.
[26] Fries N, Odic K, Conrath M, Dreyer M. The effect of evaporation on the wicking of liquids into a metallic weave. Journal of Colloid and Interface Science. 2008;321:118.
[27] Launay S, Sartre V, Lallemand M. Experimental study on silicon micro-heat pipe arrays. Applied Thermal Engineering. 2004;24:233.
[28] Duncan AB, Peterson GP. Charge optimization for a triangular-shaped etched micro heat pipe. Journal of Thermophysics and Heat Transfer. 1994;9:365.
[29] Nam Y, Sharratt S, Cha G, Ju YS. Characterization and modeling of the heat transfer performance of nanostructured Cu micropost wicks. Journal of Heat Transfer. 2011;133:101502.

Downloaded by [University of California, Los Angeles (UCLA)] at 11:16 18 April 2013